Macromolecules

ARTICLE

pubs.acs.org/Macromolecules

Osmotic Interactions, Rheology, and Arrested Phase Separation of Star−Linear Polymer Mixtures

Domenico Truzzolillo,*[,†] Dimitris Vlassopoulos,[†,‡] and Mario Gauthier[§]

[†]F.O.R.T.H, Institute of Electronic Structure and Laser, Heraklion, Crete, Greece

[‡]Department of Material Science and Technology, University of Crete, Heraklion, Crete, Greece

[§]Department of Chemistry, Polymer Research Institute, University of Waterloo, Waterloo, ON N2L 3G1, Canada

ABSTRACT:

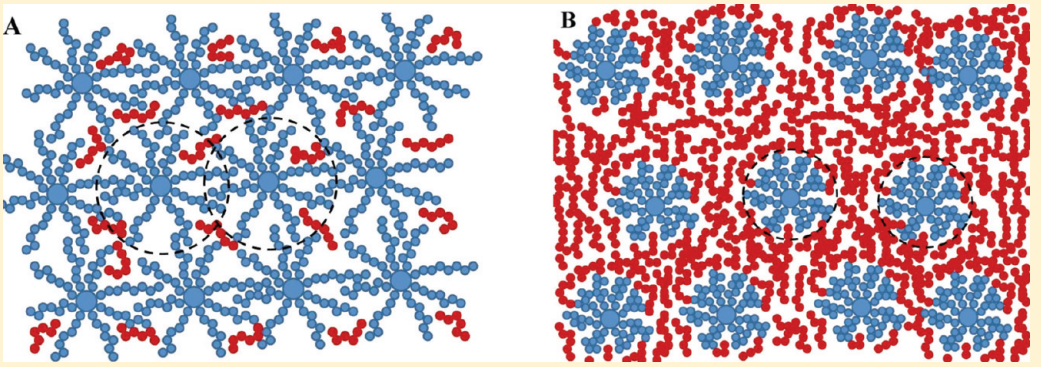

Starting from a glassy suspension of star polymers in molecular solvent, we add linear homopolymer with a fixed size ratio and ever increasing concentration, hence diluting the glass and eventually approaching the regime of stars in polymer matrix. We show that we can quantitatively decompose the rheology of the mixtures into colloidal star and linear polymer contributions by accounting for the osmotic shrinkage of the stars due to the added polymers. We also estimate the effective star overlap concentration in the mixtures and show how the rheological properties change at the crossover concentration, where the number of star-particle contacts decreases and the star repulsions weaken and eventually become attractive upon increasing the linear polymer concentration. The attraction is accompanied by a phase separation, pointing to the presence of unstable regions in the star/linear polymer phase diagram, where gelation results from an arrested phase separation. The crossover concentration is also probed by nonlinear rheological measurements. These findings are of generic nature for soft colloidal mixtures and suggest guidelines for tailoring their rheology and phase/state behavior.

I. INTRODUCTION

Colloid−polymer mixtures represent a research topic of immense scientific and technological significance. They have received a great deal of attention, particularly over the past decade with the emergence of a rigorous theoretical description of their complete phase diagram, accompanied by ample experimental evidence.[1−3] Different phases/states of the mixtures have been identified, depending on the colloid and added nonadsorbing polymer volume fractions: gas, liquid, gel, crystal, repulsive glass, and attractive glass. Their macroscopic properties (mainly rheology and diffusion) and the transitions between states have been investigated experimentally and, where possible, theoretically.[4−6]

Although "colloid−polymer mixture" is a general term, it typically refers to mixtures of hard colloidal spheres and linear nonadsorbing polymers. Yet, soft colloidal spheres have more degrees of freedom, and their behavior is very rich. Only recently, mixtures involving soft colloids and linear polymers were studied in detail.[7,8] Softness is an important parameter in these systems as it is responsible for a very rich phase behavior and associated dynamic response. It appears that the two main macroscopic reflections of softness are deformability and interdigitation. The former is a typical feature of microgel particles,[9,10] whereas the latter characterizes long hairy particles such as star polymers.[11] Of particular interest to the present work is the dense state, where colloids are glassy. The addition of linear polymers of smaller dimensions at varying size ratios and different concentrations can lead to a rich state diagram encompassing glassy, liquid, and reentrant glassy states. The key mechanism responsible for the polymer-mediated glass melting is depletion. This has been discussed at length for the case of star polymers and for varying interaction potentials.[7,12,13] In brief, there are two mechanisms associated with the osmotic effects which the added linear chains exert on the stars: shrinkage due to star deformability[14,15] and depletion.

Received: March 28, 2011
Revised: May 11, 2011
Published: May 20, 2011

Table 1. Molecular Characteristics of the Samples Used

sample code	type	total molar mass [kg/mol]	f	R^i_h (i = S, L) [nm]
S304-2	star	2100	304	16.5
L61[a]	linear	60.8	2	6.5
L165[b]	linear	165	2	13.0

[a] Obtained from Polymer Source, Canada. [b] Generously provided by Jacques Roovers.[21]

Typically, the experimental soft colloid/linear polymer systems are tertiary, as they consist of particles (the star polymers), linear polymers, and solvent molecules. One may consider, as starting point for a study, the pure star solution and add polymers in a controlled manner.[7] At the other end of the spectrum, when the molecular solvent is replaced by the polymer, we have stars in a polymer matrix which, depending on their fraction, can be thought of as a nanocomposite. The latter systems have been also studied in great detail because they possess many interesting applications.[11,16−18] Still, many problems remain unexplored. Most notably, we do not yet have clear design criteria for tailoring the properties of such complex materials at wish.

Given two extreme binary systems, such as particles in a molecular solvent, forming a colloidal glass on one hand and particles in a polymer mixture on the other hand, it is tempting to consider how they are linked, say by adding polymer to the former, how do their properties change and whether one can control the transition from colloidal glass to nanocomposite-like mixture. This could provide useful information with respect to the above-mentioned material design issue but also teach us more about the physics of these systems and possible state transformations.

In this work we take up this challenge. To this end, we use a colloidal star polymer suspension in the glassy state. We add a linear polymer at a fixed size ratio and with increasing concentration, hence moving toward the limit of a polymer matrix. We study the rheology and the physical state of the different samples (which are effectively diluted star glasses). We show how, by accounting for the osmotic effect of the polymers, we can decouple the rheology of the mixture into star and polymeric contributions. We also show that the presence of polymers alters the mixture interactions, weakening the repulsions, inducing attractions, and leading to phase separation and to a glass-to-gel transition. Nonlinear rheological data conform to the overall picture and provide further support to our findings.

The paper is organized as follows: after this brief introduction, we provide the experimental procedures in section II. Then, in section III experimental results and theoretical analysis are presented and discussed together with the observations of phase separation and their link to gelation. Finally, the main conclusions are summarized in section IV.

II. EXPERIMENTAL SECTION

II.1. Materials. We employed multiarm 1,4-polybutadiene (PBD) stars with a weight-average functionality, f, of 304 arms, and a weight-average molar mass M_w^s = 2100 kg/mol whose synthesis is described elsewhere.[19,20] We also employed linear 1,4-polybutadiene chains with two molar masses M_w^L: 60.8 and 165 kg/mol (Table 1). The polymers were dissolved in squalene, a nearly athermal, nonvolatile solvent. The hydrodynamic radii of the stars and the linear polymers were determined by dynamic light scattering in squalene at 20 °C (Table 1).

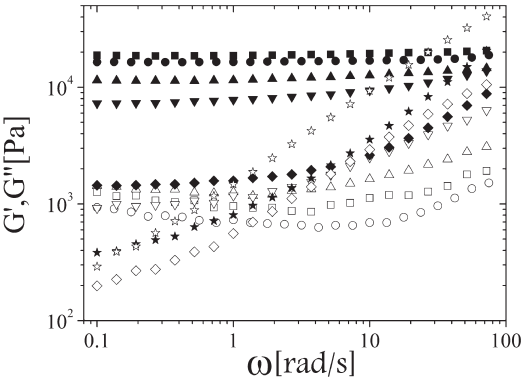

Figure 1. Storage modulus G' (filled symbols) and loss modulus G'' (open symbols) for S304-2/L61 mixtures as a function of frequency at $\gamma_0 \leq 0.5\%$ for $\Phi_s = 1.5$, $\Phi_L = 0$ (circles); $\Phi_s = 1.42$, $\Phi_L = 0.36$ (squares); $\Phi_s = 1.38$, $\Phi_L = 0.72$ (up triangles); $\Phi_s = 1.3$, $\Phi_L = 1.51$ (down triangles); $\Phi_s = 1.16$, $\Phi_L = 2.83$ (lozenges); $\Phi_s = 0.71$, $\Phi_L = 6.44$ (stars).

The size ratios δ (linear/star radius) for L61/S304-2 and L165/S304-2 are 0.39 and 0.78, respectively. The apparent colloidal volume fraction Φ_s occupied by the stars can be calculated using the measured R^s_h, the nominal molecular weight, and the measured weight fraction of the polymers in solution:

$$\Phi_s = \frac{c_s}{c^*_s} = \frac{4\pi N_A R_h^{s\,3} c_s}{3M_w^s} \quad (1)$$

where N_A is the Avogadro number and c_s is the star concentration (g/L). Initial star solutions were prepared at $\Phi_s = 1.5$, putting them in the glassy regime.[13,22] They were used to prepare the mixtures by adding increasing amount of (the two different) linear chains at constant star/solvent mass ratio, hence diluting the initial solutions. Each sample was prepared by a adding volatile cosolvent (cyclohexane) to dissolve properly the added polymers. In order to identify each mixture, we also defined the effective volume fraction of linear chains by considering only the available "free" volume in the mixture, as is typically done in hard colloid−polymer mixtures. The linear chain effective free volume fraction is defined as

$$\Phi_L = \frac{c_L}{c^*_L} = \frac{4\pi N_A R_h^{L3} c_L}{3M_w^L} \quad (2)$$

where c_L is the linear polymer concentration that only takes into account the accessible volume for linear chains, i.e., the volume of squalene contained in the mixture. The concentration of linear chains in the mixtures ranges within the following limits: $0 \leq \Phi_L \leq 6.44$ for L61/S304-2 and $0 \leq \Phi_L \leq 10.95$ for L165/S304-2.

The parameters (Φ_s, Φ_L), which univocally identify each mixture, will prove handy to quantify the osmotic effect of the chains on the star polymers.

II.2. Methods. The state of the samples was investigated with rheological measurements, which were carried out with a sensitive strain-controlled rheometer (ARES-HR 100FRTN1 from TA USA, formerly Rheometric Scientific). All the measurements were performed with a cone-and-plate geometry (stainless steel cone of 8 mm diameter and 0.166 rad cone angle). The temperature was set at 20 ± 0.1 °C with a recirculating water bath. The samples were loaded on the rheometer, and after applying a well-defined preshear protocol (200% shear amplitude oscillations at 1 rad/s for 200 s), which ensured that they were properly rejuvenated before testing,[24] their linear dynamic response was measured at different times.

The first task was to account for aging and establish conditions for reproducible and virtually time-independent measurements. Typically, the time scale for this was about 1 day. Subsequently, small-amplitude

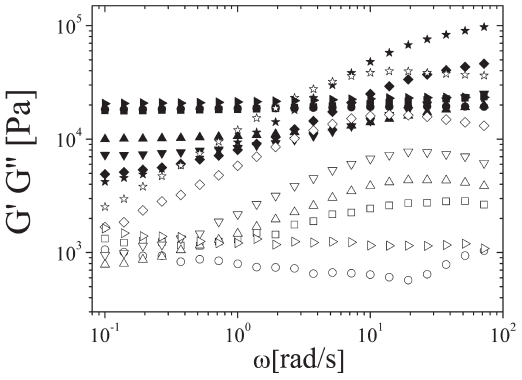

Figure 2. Storage modulus G' (filled symbols) and loss modulus G'' (open symbols) for S304-2/L165 mixtures as a function of frequency at $\gamma_0 \leq 0.5\%$ for $\Phi_s = 1.5$, $\Phi_L = 0$ (circles); $\Phi_s = 1.48$, $\Phi_L = 0.20$ (right triangles); $\Phi_s = 1.46$, $\Phi_L = 0.85$ (squares); $\Phi_s = 1.38$, $\Phi_L = 2.15$ (up triangles); $\Phi_s = 1.3$, $\Phi_L = 4.38$ (down triangles); $\Phi_s = 1.20$, $\Phi_L = 7.55$ (lozenges); $\Phi_s = 1.05$, $\Phi_L = 10.95$ (stars).

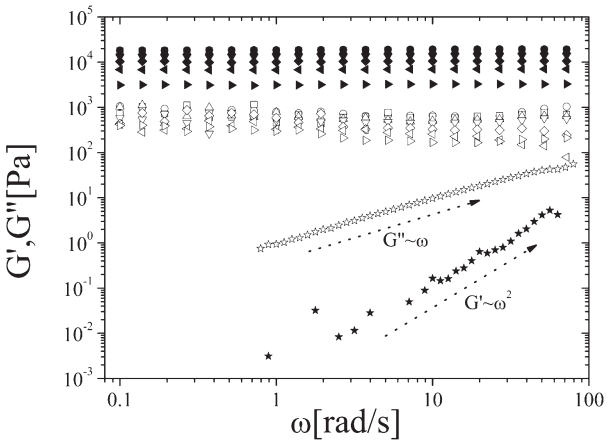

Figure 3. Storage modulus G' (filled symbols) and loss modulus G'' (open symbols) for S304-2 solutions as a function of frequency at $\gamma_0 \leq 0.5\%$ for $\Phi_s = 1.5$ (circles); $\Phi_s = 1.48$ (squares); $\Phi_s = 1.46$ (up triangles); $\Phi_s = 1.30$ (down triangles); $\Phi_s = 1.15$ (lozenges); $\Phi_s = 1.07$ (left triangles); $\Phi_s = 0.9$ (right triangles); $\Phi_s = 0.8$ (stars).

oscillatory shear tests were carried out in the frequency range 0.1−100 rad/s. Nonlinear measurements were also performed on these mixtures. In particular, large-amplitude oscillatory shear (LAOS) was accomplished via dynamic strain sweep tests which were carried out at a fixed frequency (1 rad/s) with strain amplitudes covering the range from the linear (≤0.5%) to the strongly nonlinear (250%) regime.

III. RESULTS AND DISCUSSION

III.1. Linear Viscolelasticity. The linear viscoelestic spectra of the various star/linear mixtures were obtained using frequency sweep measurements with low-amplitude strain. The frequency dependences of the loss (G'') and storage moduli (G') are depicted in Figures 1 and 2 for the two different linear polymers used, L61 and L165, respectively. In the absence of linear chains, the concentrated star solution with an apparent volume fraction $\Phi_s = 1.5$ exhibits a glasslike behavior with G' and G'' being only weakly frequency-dependent and $G'(\omega) > G''(\omega)$ over the 3 decades of frequency investigated. Upon addition of linear chains at increasing concentrations, both moduli become more and more sensitive to frequency variations. The decrease in G' at low frequencies and the rise of both G' and G'' at high frequencies become more clearly observable as the linear chains content increases. Note however that, despite the change in viscoelastic response, the eventual solidlike behavior persists throughout the range of linear chains concentrations investigated here. At the lowest frequencies $G'(\omega)$ exceeds $G''(\omega)$ and remains nearly independent of ω. The dilution of the initial star solution ($\Phi_s = \Phi_0 = 1.5$) down to $\Phi_s < 1.3$ due to the added linear chains L61 causes the loss of the characteristic glassy concave shape[25] of $G''(\omega)$ in the frequency range examined (with G' being nearly constant) and the concomitant sensible decrease of the storage modulus at low frequencies for $1.15 < \Phi_s < 1.3$. The same behavior is also present in the case of the higher molar mass L165 but somewhat less pronounced, presumably because of the higher viscoelasticity of the polymer matrix surrounding the glassy star polymer suspension. As seen in Figure 2, for $1.05 < \Phi_s < 1.3$ and $\omega < 10$ rad/s G' decreases very weakly with decreasing frequency, whereas G'' exhibits a stronger dependence with an approximate power law of $G''(\omega) \sim \omega^{0.7}$.

In order to compare the rheology of the mixtures with the behavior of the one-component star polymer system at different concentrations, we show in Figure 3 the frequency dependence of the loss and storage moduli of star polymer solutions in squalene for $0.8 \leq \Phi_s \leq 1.5$. We show how, upon the dilution, the nearly frequency-independent moduli (G' and G'') decrease until the liquid state is reached for $\Phi_s = 0.8$ where the terminal power laws ($G' \sim \omega^2$ and $G'' \sim \omega^1$) are evidenced.

Through the comparison with the one-component solutions, we conclude that the high-frequency behavior of the mixtures should reflect the response of the polymer matrix, which can be viewed as the "the effective solvent" for the star polymer suspension. Indeed, the high-frequency (9 rad/s) $G'-G''$crossover of the mixture (at $\Phi_s = 1.05$), containing the larger molar mass linear polymer (L165), is identical to the terminal crossover of the polymer matrix effectively confined in the space among stars. In order to test this scenario, we performed linear viscoelastic measurements on pure linear chains L165 in squalene at the same concentration as in the mixture within the free space excluding the stars. When the size of the linear chains is comparable to that of the stars, having a high number of arms, it is reasonable to assume that the penetration of chains within the stars' spherical concavity is limited as this process involves a significant loss of entropy.[26−30] In Figure 4 we provide a comparison between the rheological results obtained from the star/linear polymer mixture S304-2/L165 at $\Phi_s = 1.05$ and from two linear polymer solutions at different concentrations. The first linear polymer solution, having the same linear polymer-to-solvent mass ratio as the star−linear polymer mixture ($\Phi_L = 10.95$), does not display a good agreement with the mixture's dynamic frequency sweep in the high-frequency regime, showing a high-frequency $G'-G''$ crossover at $\omega \approx 27$ rad/s as compared to 10 rad/s for the mixture (see arrows in Figure 4). This discrepancy reflects the effect of the confinement of the chains within the star polymer suspension. To confirm our claim, we prepared more concentrated solutions of linear polymers in order to match the high-frequency moduli of the mixture. In addition, we estimated the accessible volume for the chains, the volume occupied by the stars as well as their shrinkage. As shown in Figure 4, we obtained a good

dx.doi.org/10.1021/ma2007078 |*Macromolecules* 2011, 44, 5043–5052

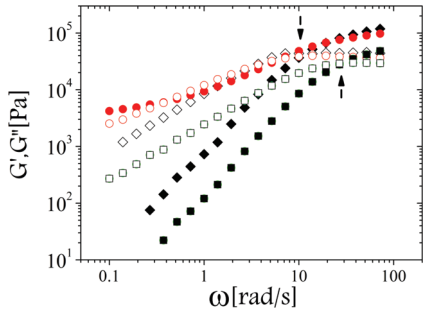

Figure 4. Storage modulus G' (filled symbols) and loss modulus G'' (open symbols) as a function of frequency at $\gamma_0 \leq 0.5\%$ for S304-2/L165 mixture at $\Phi_s = 1.05$ (stars) (red circles); 165 kDa linear polymer solution $\Phi_L = 10.9$ (squares); 165 kDa linear polymer solution $\Phi_L = 14.5$ (lozenges). The arrows indicate the crossover frequency between G' and G''.

agreement between the linear polymer solution and the mixture for the high-frequency moduli for $\Phi_L = 14.0$.

Given this value of concentration, we calculated the effective volume occupied by the chains, the volume occupied by a single star molecule, defined as the volume that is inaccessible to the linear polymers, and hence, we estimated the effective radius of the star polymers within the mixture using the known experimental quantities:

$$R_s = \left(\frac{3\left(V_T - \frac{W_L}{\Phi_L c^*_L}\right) M^s_w}{4\pi W_s N_A} \right)^{1/3} \quad (3)$$

Here W_L and W_s are respectively the mass fractions of linear chains and star polymers within mixtures having a total volume V_T.

We obtained $R_s = 0.58R^s_h$. The same procedure has been repeated for the mixture S304-2/L165 at $\Phi_s = 1.20$: we obtained $R_s = 0.67R^s_h$.

As discussed later, these values agree with those determined on the basis of the osmotic shrinkage of the stars in presence of linear chains. Therefore, it is possible to have a direct rheological evaluation of the osmotic pressure effect exerted by linear homopolymer chains on star polymers in concentrated dispersions. The rationalization of this effect, i.e., the analysis of the osmotic star shrinkage, follows in the next section.

III.2. Osmotic Shrinkage: Theoretical Analysis. The size of an isolated star polymer molecule in a matrix of linear chains can be evaluated by employing the Flory argument,[14,31−34] accounting for the osmotic pressure contribution of the chains that depends on their volume fraction $\Phi_L = c_L/c_L^*$. The insertion of a star polymer in a solution of linear chains gives rise to the expulsion of the latter from a region of size R.[14] The free energy cost for creating such a cavity corresponds to the mechanical work that has to be done in order to open a spherical free space within the solution:

$$F_{os}(R) = \frac{4\pi}{3} R^3 \Pi(\Phi_L) \quad (4)$$

where Π is the osmotic pressure exerted by the polymer matrix. Because of the penetrability of the star polymer molecules, we can neglect the surface term. In fact, the transition of the polymer concentration from the average value in the solution to its value within the star interior is gradual,[14,31] thereby minimizing the interfacial cost.

The other terms of the free energy for a single star of radius R_s that we have to take into account are the elastic and the interaction free energy given by[31]

$$F_{el}(R) = k_B T \frac{3f{R_s}^2}{2N_s a^2} \quad (5)$$

$$F_{int}(R_s) = k_B T \frac{\upsilon {N_s}^2 f^2}{2N_s a^2} \quad (6)$$

where k_B is the Boltzmann constant, T the temperature, a the length scale of monomers, N_s the degree of polymerization of the arms, and υ the excluded-volume parameter.

We will employ for simplicity $\upsilon = 1$, which is appropriate for a good solvent.[14] The competition between the osmotic interaction and elastic contribution can only lead to shrinkage of the star with respect to the free-chain case because the pressure grows with R.

Note that the radius of the cavity appearing in eq 4 does not necessarily correspond to the radius of gyration R_s because of the penetrability of the stars. Camargo and Likos recently showed[35] that chains around a star can penetrate the latter up to a distance $\sigma = {}^4/_3 R_s$ for a wide range of size ratios, so that we can write $R = bR_s$ with $b = 1.3$.[14] The size ratio between chains and stars is defined as $\delta = R_L/R_s$, where R_L is the radius of gyration of the linear chains. Furthermore, within the canonical ensemble renormalization group formalism for a semidilute monodisperse polymer solution in 3 dimensions, the osmotic pressure dependence on polymer concentration has been found[14,36]

$$\Pi(\Phi_L) = \frac{k_B T}{c_L}[1 + P(\Phi_L)] \quad (7)$$

where

$$P(x) = \frac{1}{2} x \exp\left\{ \frac{1}{4}\left[\frac{1}{x} + \left(1 - \frac{1}{x}\right) \ln(x+1) \right] \right\} \quad (8)$$

and

$$x(\Phi_L) = \frac{1}{2}\Phi_L \pi^2 \left[1 + \frac{1}{4}\left(\ln 2 + \frac{1}{2} \right) \right] \quad (9)$$

Thus, minimizing the total free energy with respect to R_s, we obtain

$$\frac{3faR_s}{N_s} + 4\pi b^3 {R_s}^2 \delta^{-3} {N_s}^{-3\nu} f^{-3/5} \Phi_L [1 + P(\Phi_L)] - \frac{3\upsilon {N_s}^2 f^2 a^3}{2{R_s}^4} = 0 \quad (10)$$

where we have used the scaling relation $\delta = (1/f^{1/5})(N_c/N_s)^{\nu}$[31] and the simple relation defining the overlap number concentration ${c_L}^* = a^{-3} {N_c}^{-3\nu}$ with $\nu = 3/5$ the Flory exponent. By solving eq 10, we can predict the reduction factor $g = R_s/R_0$ for a star polymer, with the radius R_0 being the chain-free value of the (pure) star in infinitely dilute solution. As first quantitative test of the theoretical prediction, we compare the values of g obtained via linear viscoelastic spectra, as described in section III.2, with the value calculated through eq 10 assuming the known data for the stars and linear chains employed here ($f = 304$, $a = 0.5$ nm,[37,38] $N_s = 125$, $\delta = 0.78$); we obtain a very good agreement: $g = 0.60$ for $\Phi_s = 1.05$ and $g = 0.71$ for $\Phi_s = 1.20$ (see Figure 6A). Using the 3D-osmotic theory as theoretical tool,

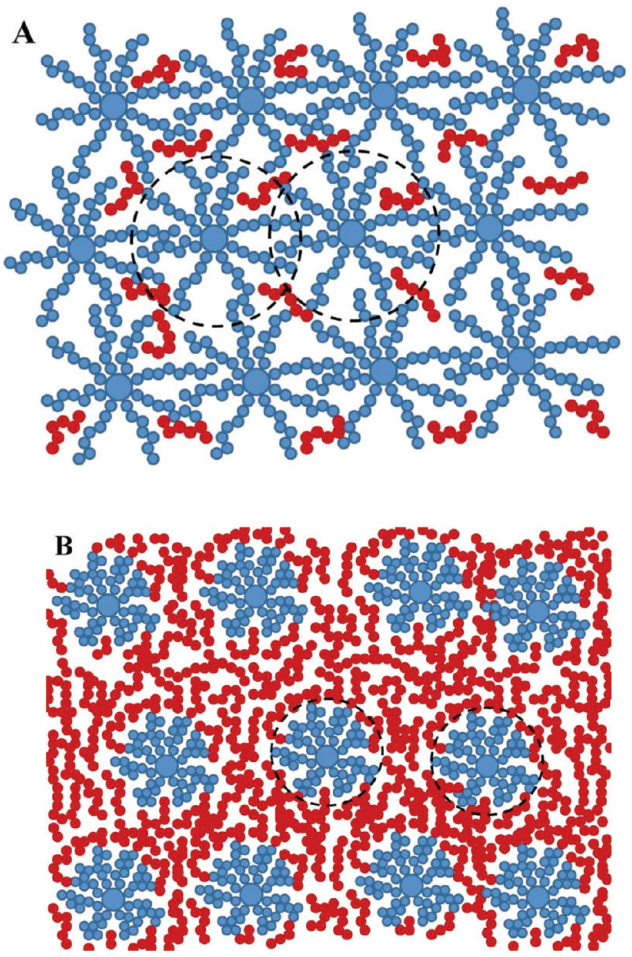

Figure 5. Sketch of the two regimes in star/linear polymer mixtures. Panel A: $\Phi_s > \Phi^*$ where $d_s < 0$. Panel B: $\Phi_s < \Phi^*$ where $d_s > 0$. Dashed lines represent the (2D) ideal surfaces of star polymers.

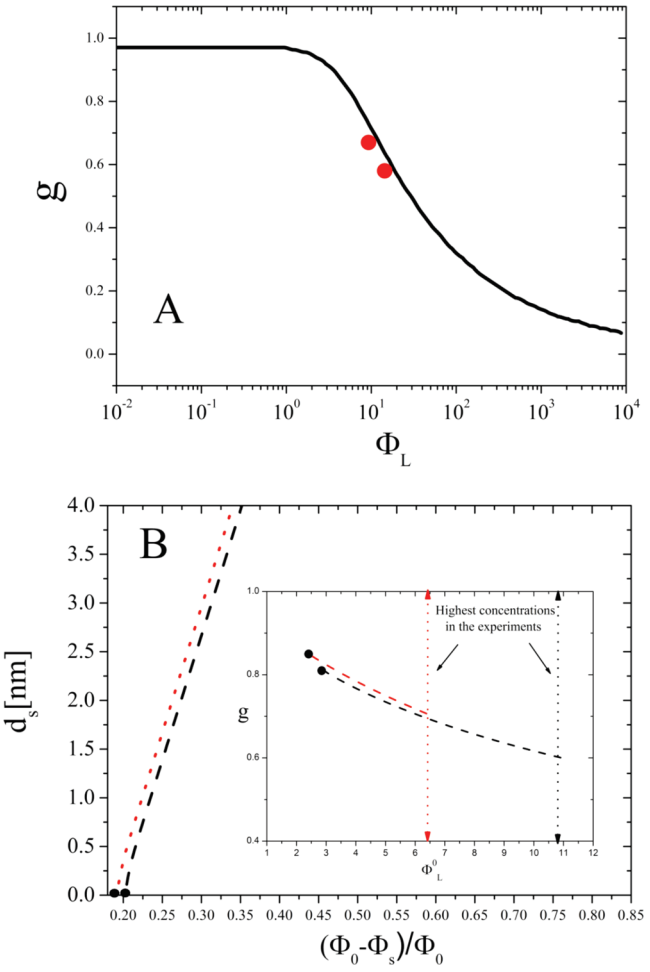

Figure 6. Theoretical analysis via osmotic theory. Panel A: comparison between the values of the reduction factor $g = R_s/R_0$ obtained from linear viscoelastic spectra (red points) (see section III.1) and the theoretical dependence g vs Φ_L calculated from eq 10 (straight line) for $\delta = 0.78$, $f = 304$, $N_s = 125$, $a = 0.5$ nm. Panel B: mean star surface−surface distance as a function of $(\Phi_s - \Phi_0)/\Phi_0$ calculated from eq 11 solving recursively eqs 10 and 13 for both the size ratios $\delta = 0.39$ (black dashed line) and $\delta = 0.78$ (red dotted line). Inset: calculated value of g as a function of the linear polymer concentration Φ_L^0; the black points correspond to the overlap-to-nonoverlap transition ($d_s = 0$); the dotted lines indicate the highest values of linear chains concentration in the mixtures (red: S304-2/L61; black: S304-2/L165).

we can also explain the subtle change in the frequency spectra in the range $1.05 < \Phi_s < 1.3$ of Figure 2 and $0.71 < \Phi_s < 1.3$ of Figure 1, respectively. The latter will be also discussed within the context of nonlinear rheology measurements below.

A closer look at the problem suggests in fact that the addition of linear chains to the concentrated star solution involves two different "dilution" mechanisms. The first one is geometric in nature and is due to the obvious increase of the total volume of the solution causing an increase of the center-to-center distance between the stars. On the other hand, the second mechanism is directly connected to the osmotic reduction of the radius of the stars upon adding chains, yielding a further separation between the ideal star surfaces. The surface-to-surface distance d_s can be written in function of the star volume fraction Φ_s and the effective linear polymer fraction Φ_L as follows:

$$d_s = R_0 \sqrt[3]{\frac{4\pi}{3\Phi_s}} - 2g(\Phi_L)R_0 \qquad (11)$$

where

$$\Phi_L = \frac{\rho_L}{c^*_L}\left(1 - \frac{\Phi_s}{\Phi_0}\right) \qquad (12)$$

Here ρ_L (890 mg/mL[39]) and c_L^* are the density and the overlap concentration of the linear 1,4-polybutadiene chains, respectively, and Φ_0 is the initial volume fraction of the star polymers in the free-chains solution.

Though eqs 10, 11, and 12 allow us to estimate the radius of star polymers for different values of Φ_s so that we could, in principle, calculate the concentration of star polymers when $d_s = 0$, i.e., the concentration where the disengagement of the stars occurs, the effective volume fraction of chains and the size of stars must be self-consistently evaluated.

Up to the disengagement concentration (i.e., for $d_s \leq 0$), the behavior of the star−linear polymer mixture is strongly dominated by the star dynamics, since the isolated and confined linear chains do not qualitatively affect the rheology. In this regime, the Flory argument-based theory cannot be applied, and the reduction of the average star polymer size is mainly affected by the

specific repulsion between stars because of the overlap of their outer blobs. Under these conditions its dependence on the presence of few isolated chains cannot be estimated easily via mean-field approaches.

On the other hand, for $d_s > 0$, the formation of a spherical cavity is geometrically well-defined as well as is the surrounding polymeric medium, and hence the osmotic pressure can be calculated. Thus, holding this condition, we can extend the osmotic theory to concentrated star polymer solutions. This is clearly a departure from ref 14 which only considers the shrinkage problem for a single star.

In this regime, we emphasize that the mixtures lose their typical glassy behavior and the linear polymer matrix appears to dominate the response (Figure 5A,B illustrates the two regimes). It is worth noting that all the mixtures studied are viscoelastic solids even at the lowest star volume fraction ($\Phi_s = 0.71$), which is below the volume fraction, Φ_{GL}, where the glass-to-liquid transition occurs for pure S304-2 solutions ($0.8 < \Phi_{GL} < 0.9$) (for details see section III.4).

To quantify the above ideas, we need to consider the fact that, when a certain mass fraction W_L of linear polymer chains is added to a star polymer solution, the confinement of the chains caused by the presence of shrunk stars has to be taken into account in order to evaluate the effective volume fraction Φ_L. This leads to

$$\Phi_L = \frac{W_L \Phi_L^0}{W_L + \frac{W_s \Phi_L^0 c^*_L}{\rho_s} - \frac{4}{3}\pi N_s \Phi_L^0 c^*_L R_s^3} \qquad (13)$$

where N_s is the total number of star polymers in the solution, Φ_L^0 is the volume fraction of chains calculated taking into account the total volume of the solvent (squalene), and ρ_s is the density of the star polymer melt. We solved recursively eqs 10 and 13 until converging to stable values (Φ_L, R_s) of linear chain volume fraction and star polymer dimension that univocally define the mixture and definitely allow to estimate the mean distance between ideal surfaces of stars according to eq 11. Figure 6B depicts the calculated distance between stars as a function of the dilution parameter $\varepsilon = (\Phi_0 - \Phi_s)/\Phi_0$ for the two star−linear polymer mixtures employed here. The inset shows the correspondent values of g as a function of the linear polymer concentration Φ_L^0. The condition $d_s = 0$ is obtained for $\delta = 0.39$ at $\varepsilon \approx 0.20$ and for $\delta = 0.78$ at $\varepsilon \approx 0.18$ that correspond to $\Phi_s = \Phi^* = 1.2$ and $\Phi_s = \Phi^* = 1.23$, respectively. These volume fractions can be viewed as the *renormalized overlap concentrations* for star polymer molecules within the mixtures and corroborate the scenario emerging from the analysis of the linear viscoelastic data. This analysis definitely generalizes and extends the theory of Wilk et al.[14] to concentrated star polymers solutions, hence identifying the departure from the dilute regime.

Moreover, as discussed in the next section, this scenario is also consistent with the nonlinear rheological properties of these mixtures, which are surprisingly sensitive to the transition between the overlapping and nonoverlapping stars regimes just described.

III.3. Nonlinear Rheology. Strain-amplitude sweep tests were conducted in order to characterize the behavior of the mixtures under large deformations. Figure 7 presents indicative results for the star/linear mixtures containing different amounts of L61 chains. In particular, it depicts the variation of the first harmonics of G' (Figure 7A) and G'' (Figure 7B) with increasing strain amplitude γ_0 at $\omega = 1$ rad/s. As expected, for small amplitudes, both moduli are insensitive to the amplitude of the applied strain: the sample obeys linear viscoelastic response. At larger strains, $G''(\gamma_0)$ increases (apparent thickening) and reaches a maximum G_M'' before eventually declining. At the same time, $G'(\gamma_0)$ decreases with strain smoothly and eventually obeys a power law. In this regime the material begins to yield and switches from solidlike ($G' > G''$) to liquidlike ($G'' > G'$).

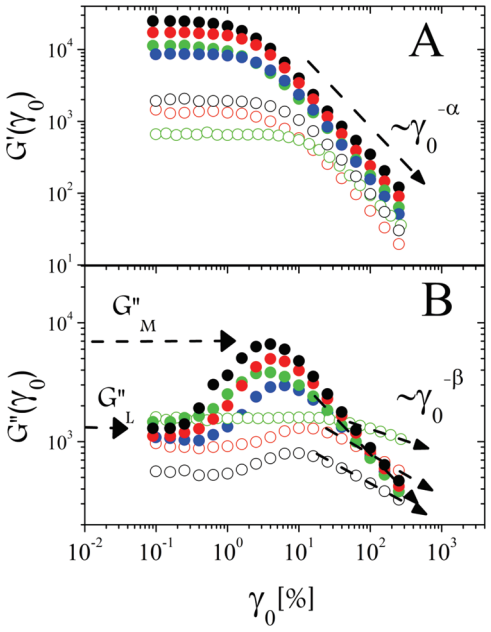

Figure 7. Dynamic strain sweeps measurements for S304-2/L61 mixtures and $0.1\% \le \gamma_0 \le 250\%$. Filled points → $\Phi_s > \Phi^*$; empty points → $\Phi_s < \Phi^*$: Panel A: storage modulus G': $\Phi_s = 1.47$ (black filled circles), $\Phi_s = 1.42$ (red filled circles), $\Phi_s = 1.38$ (green filled circles), $\Phi_s = 1.3$ (blue filled circles), $\Phi_s = 1.16$ (black empty circles), $\Phi_s = 1.08$ (red empty circles), $\Phi_s = 0.72$ (green empty circles). Panel B: loss modulus G'': $\Phi_s = 1.47$ (black filled circles), $\Phi_s = 1.42$ (red filled circles), $\Phi_s = 1.38$ (green filled circles), $\Phi_s = 1.3$ (blue filled circles), $\Phi_s = 1.16$ (black empty circles), $\Phi_s = 1.08$ (red empty circles), $\Phi_s = 0.72$ (green empty circles); the low strain loss modulus value G_L'' and its maximum value G_M'' are marked by dashed arrows for $\Phi_s = 1.47$, while differently sloping arrow outline the passage from the concentrated regime (invariance of the slope $-\beta$) for $\Phi_s \ge 1.3$, to the diluted regime (dependence of the slope by the linear chain's content) for $\Phi_s \le 1.16$.

The power-law behaviors are $G'(\gamma_0) \sim {\gamma_0}^{-\alpha}$ and $G''(\gamma_0) \sim {\gamma_0}^{-\beta}$ where α and β values depend on the linear polymer content of the mixtures. For many soft matter systems,[10,23,40−46] the ratio α/β was reported to be nearly constant, reaching a value of 2, which was recently rationalized by invoking a modified mode coupling theory approach that incorporates the notion of a rate-dependent characteristic time of the material.[40,47] This can be also predicted from the soft glassy rheology model.[48] We obtained the α and β values by fitting the data for $\gamma_0 \ge 75\%$ where it has been shown that a complete fluidization of similar star polymer glasses occurred[22,24] and both G' and G'' no longer depend on the initial state.

Interestingly, the qualitative behavior of the moduli is maintained for $\Phi_s > 1.30$ while for lower volume fractions an abrupt decrease of the low strain storage modulus is evidenced together with the concomitant change of three characteristic features of the moduli spectra: the ratio α/β, the relative apparent thickening $(G_M'' - G_L'')/G_L''$, where G_L'' is the value assumed by the loss modulus in the linear regime and the strain position of the

dx.doi.org/10.1021/ma2007078 |*Macromolecules* 2011, 44, 5043–5052

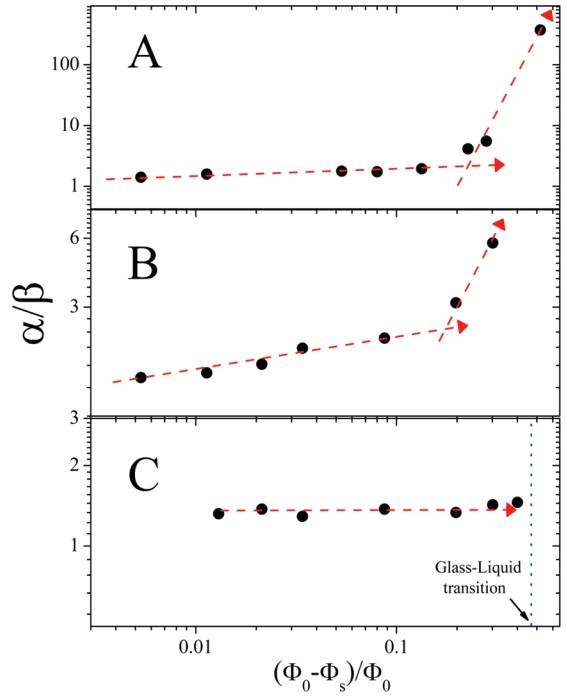

Figure 8. Ratio α/β for both S304-2/L61 (panel A) and S304-2/L165 (panel B) mixtures. Panel C shows α/β for the one-component star polymer solutions at different concentrations. Dashed red arrows are only a guide for the eye to locate the "crossover" value $(\Phi_0 - \Phi^*)/\Phi_0$.

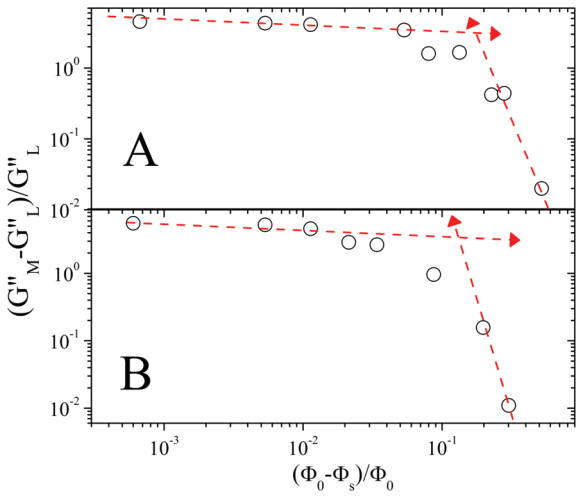

Figure 9. Relative apparent thickening $(G_M'' - G_L'')/G_L''$ for both S304-2/L61 (panel A) and S304-2/L165 (panel B) mixtures. Dashed red arrows are only a guide for the eye to locate the "crossover" value $(\Phi_0 - \Phi^*)/\Phi_0$.

maximum in the G'' spectrum γ_M. Figure 8 depicts the ratio α/β for all the two star/linear mixtures investigated and for the star polymer solutions in squalene at different concentrations. We show how for both mixtures this ratio slightly depends on the polymer concentration until a critical value of Φ_s is reached. In particular we show how an unambiguous change of slope occurs for $\varepsilon \approx 0.2$ for both S304-2/L165 and S304-2/L61 mixtures that immediately brings us back to the comparison with the overlap concentration predicted by 3D-osmotic theory (section III.2).

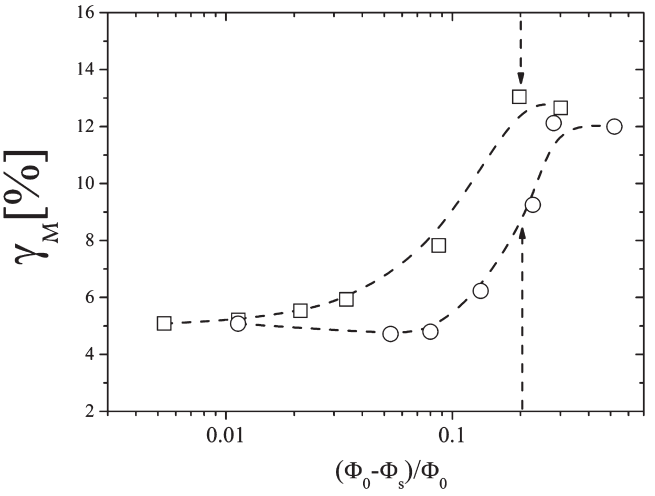

Figure 10. Strain amplitude γ_M correspondent to the maximum of $G''(\gamma_0)$ for both S304-2/L61 (circles) and S304-2/L165 (squares) mixtures. The values have been obtained via parabolic fits of the data close to the measured maximum.

The change of slope is absent in the pure star polymer solutions corroborating the idea that the appearance of the crossover concentration is induced by osmotic effects. However, it is important to note that the dramatic increase of the ratio α/β may also reflect the fact that in the star/linear mixtures the terminal slope (at large strains) has not been reached in the experimental window investigated.

At the same time, we report in Figure 9 the change of the relative apparent thickening taking place when varying the linear polymer content where we verify the existence of a crossover appearing in the same range of ε mentioned before. Furthermore, Figure 10 shows the strain amplitude γ_M where G'' reaches its maximum (evaluated via parabolic fits of the data close to the measured maxima) as a function of ε. Once again, the data for both mixtures display a sharp increase that appears to level off around $\varepsilon \approx 0.2$ (see dashed arrows in Figure 10). We will comment briefly on the above-mentioned phenomenological evidence in an effort to elucidate the origin of the observed behavior.

The dilution of a glassy soft particle solution trough the addition of linear chains can be viewed as the natural way to investigate the transition of soft matter from colloidal glasses to linear polymer melts, expecting to find the pure melt behavior in the limit of very high chains' content ($\varepsilon \rightarrow \infty$). When we add chains to a crowded star polymer system, they can assume, in principle, very different conformations according to the functionality and volume fraction of stars. When confined chains are isolated ($\varepsilon \ll 1$), the glassy response of the mixtures is preserved and the presence of chains within the solution can be detected by looking at the high-frequency regime of dynamic frequency sweeps, where the fastest modes reflect the polymer matrix response (also well below the overlap-to-nonoverlap transition of stars). In this regime, increasing the amplitude of the imposed strain does not induce any significant change in the elastic and viscous properties of mixtures. The qualitative characteristics of the pure glassy star polymer solution [α/β ratio, relative apparent thickening, and $\gamma_M(\varepsilon)$] remain unchanged. However, as the star polymer molecules disengage, the star−star interactions drop while the confined chain−chain interactions radically

dx.doi.org/10.1021/ma2007078 |*Macromolecules* 2011, 44, 5043–5052

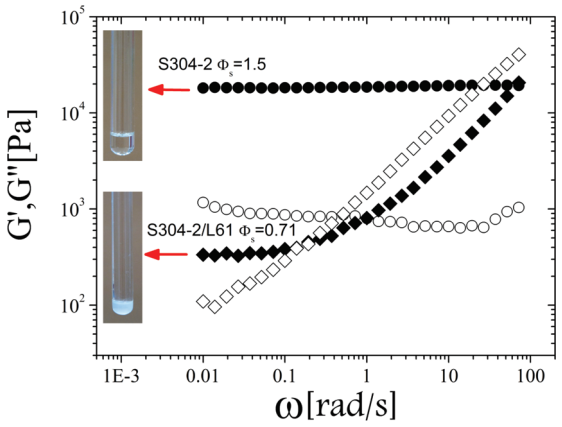

Figure 11. Storage modulus G' (filled symbols) and loss modulus G'' (open symbols) for pure glassy star polymer solution S304-2 $\Phi_s = 1.5$ (circles) and mixture S304-2/L61 $\Phi_s = 0.71$ (lozenges). Right panels: correspondent images of the samples.

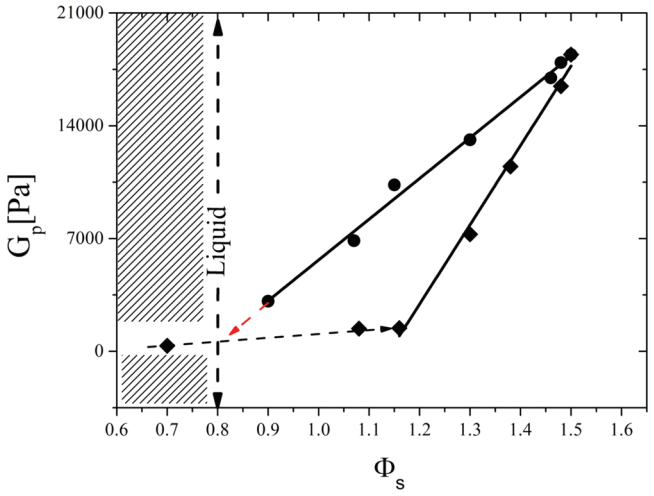

Figure 12. Storage modulus G_p' for $\omega \leq 0.1$ rad/s of different pure star polymer solutions S304-2 in the range $0.8 \leq \Phi_s \leq 1.5$ (circles) and of mixtures S304-2/L61 in the range $0.71 \leq \Phi_s \leq 1.5$ (lozenges). The solid black lines represent the best linear fit on the data for $0.9 \leq \Phi_s \leq 1.5$ (pure star polymer solutions S304-2) and for $1.15 \leq \Phi_s \leq 1.5$ (mixtures S304-2/L61). At $\Phi_s = 0.8$ the pure star polymer solution becomes rheologically liquid. The dashed arrows are only a guide for the eye.

start contributing to the yielding and the shear thinning of the material. As the stars become eventually virtually "isolated" ($d_s > 0$) and immersed in the concentrated polymer solution, the material can be viewed as stars in solution of linear chains with varying interaction. This is demonstrated by the linear viscoelastic spectra described in Figure 4 and by the fact that the soft colloidal suspensions exhibit solidlike behavior in the low-frequency window of the spectra.

III.4. Phase Separation and Gelation. As mentioned in section III.2, we surprisingly obtained a viscoelastic solid even at a volume fraction ($\Phi_s = 0.71$) that is lower than the glass-to-liquid transition found for pure S304-2 star polymer solution.

The latter was found to be in the range $0.8 < \Phi_{GL} < 0.9$, as roughly estimated by simply diluting the initial glass with squalene until the liquid phase was recovered. In Figure 11 we show the linear storage and loss moduli over a wider range of frequencies (0.01 rad/s $< \omega <$ 100 rad/s) in order to distinguish the different type of solidlike behavior of the mixture S304-2/L61 at $\Phi_s = 0.71$ from that of the original glassy system. It is important to point out that this value of the concentration of the soft colloidal particles within the mixture should be considered only as an upper bound for their effective packing fraction because it does not take into account for the osmotic reduction of their sizes due to the presence of the surrounding concentrated linear chains solution.[14] Using the osmotic theory-based calculation described in section III.2, we obtain $g = 0.55$, hence predicting an effective volume fraction of stars $\Phi_e = g^3\Phi_s = 0.12$. However, there is evidence that, at this concentration, the system undergoes macroscopic phase separation with a huge increase of the turbidity of the solution. This is in fact visible to the eye. The two pictures shown in Figure 11 display the pure star polymer glass $\Phi_s = 1.5$ and the mixture S304-2/L61 $\Phi_s = 0.71$ in NMR tubes after 1 day after sample preparation. They clearly show the optical difference between the two samples: the opacity of the mixture is much higher than the pure star polymer solution, the latter appearing transparent, signaling the occurrence of a phase separation upon adding linear chains in the original solution.

Figure 12 provides a comparison of the low-frequency plateau moduli $G_p(\Phi_s)$ for the simple glassy star solutions at different concentrations and for S304-L61 mixtures. In the case of simple dilution of the initial glassy system ($\Phi_0 = 1.5$), G_p shows a pure linear dependence on Φ_s as already shown in other star polymer systems,[23] until the liquid phase is reached ($\Phi_s = 0.8$). The respective dependence of the storage modulus of the mixtures clearly follows two regimes: the first, at low linear polymer content, is characterized by a linear decrease upon the addition of chains, where a steeper slope with respect to the pure stars' solutions corroborates the idea that a reduction of the effective volume of single stars follows the addition of chains. The second regime is characterized by a weaker dependence on Φ_s leading eventually to a solidlike response even for a concentration where a liquid is expected. This scenario conforms to the idea that above a well-defined concentration of linear chains, corresponding to the stars overlap-to-nonoverlap crossover concentration, the interactions between the stars progressively weaken[7,15] and eventually switch from repulsive to strongly attractive in the presence of a concentrated solution of relatively small chains, leading the system to gelation. Recently, Camargo and Likos[49] showed that for stars of low functionality ($f = 18$) and size ratio $\delta = 0.5$ a cluster prepeak appears in the static structure factor of coarse-grained modeled star−linear polymer mixtures, signaling the presence of a preferential cluster size as a precursor for a demixing transition. On the other hand, increasing f, the cluster prepeak disappears and the system is directly driven to the demixing transition as the concentration of the chains is increased.[15] Their findings support the existence of macrophase separation in such mixtures and corroborate our experimental results.

Furthermore, it is worth noting that in our case the demixing transition appears with a persistent dynamical arrested state of the system, which presumably leads to a glass-to-gel boundary in the phase diagram of star/linear polymer solutions.

Thermodynamic models considered gelation initiated by fluid−crystal[50] or liquid−gas phase separation[51,52] which may arrest leading to percolation. Interestingly, Lu et al.[53] interestingly provided strong quantitative physical evidence that the gelation boundary for short ranged attractive particles is precisely

equivalent to the boundary for equilibrium liquid−gas phase separation in low-density solutions. While, such polymer−hard sphere mixtures can be easily parametrized with three mutually independent quantities, namely the packing fraction of colloids Φ, the attraction strength U/k_bT and the range of the attraction ξ, the star−linear polymer systems contain a much higher "degree of complexity" because of the pronounced interdependence of the three above-mentioned parameters, so that they cannot be easily represented via the existing coarse grained models aiming to capture the details of the phase diagram.

The deformability of the star polymers, even with a large number of arms, giving, as postulated here, a strong dependence of the size of particles on the chains' content, makes reasonable a sharp passage from a glassy state, dominated by repulsive interactions and characterized by both in-cage and out-of-cage dynamics,[43] to a low-density attractive gel phase, where percolation stops the growth of the clusters and phase separation, whereas at the same time the osmotic constraints, imposed by the very dense linear polymer solution, render the stars smaller and hard-sphere-like.

IV. CONCLUDING REMARKS

We have investigated the rheological behavior of star/linear polymer mixture employing two different molar mass of linear chains (of the same chemical nature) to dilute a concentrated glassy solution of star polymers. We have shown that the dilution of the initial glassy phase is reflected in the lower low-frequency storage modulus of the material (depending on the size ratio) as well as the fact that the high-frequency moduli are dominated by the linear chains contribution. We directly estimated the reduction of the size of the stars upon the addition of chains comparing the results with those obtained via osmotic theory. We used the latter to estimate the effective overlap concentration of stars in the mixtures showing how the rheological properties change close to the crossover concentration, where the number of contacts between the particles per unit time and volume sharply decreases and the particle−particle interaction potential changes from purely repulsive to weakened repulsive and eventually become attractive, in the presence of high concentration of chains. We have underlined how a macroscopic phase separation occurs in the mixtures containing the chains with the smallest molar mass employed here (60.8 kg/mol), together with a persistent solid (gel-like) state even below the solid-to-liquid transition corresponding to the pure star solutions. This finding suggests the presence of unstable regions in the star/linear polymer mixtures phase diagram where an arrested phase separation (demonstrated here by simple visual observation) guides the gelation of the ultrasoft colloidal particles. This provides new possibilities for tailoring the macroscopic properties of soft colloids and hence for further experimental investigations.

AUTHOR INFORMATION

Corresponding Author

*E-mail: truzzoli@iesl.forth.gr.

ACKNOWLEDGMENT

Financial support from the EU (ITN-COMPLOIDS, FP7-234810) is gratefully acknowledged. We thank Antje Larsen for help in the DLS characterization of the star and linear polymers employed. D.T. thanks Andreas Poulos, Nikos Koumakis, Rossana Pasquino, and Frank Snijkers for fruitful discussions. M.G. acknowledges the financial support of the Natural Science and Engineering Research Council of Canada (NSERC).

REFERENCES

(1) Pham, K. M.; Puertas, A. M.; Bergenholtz, J.; Egelhaaf, S. U.; Moussaiud, A.; Pusey, P. N.; Schofield, A. B.; Cates, M. E.; Fuchs, M.; Poon, W. C. K. *Science* **2002**, *296*, 104–106.

(2) Pham, K. N.; Egelhaaf, S. U.; Pusey, P .N.; Poon, W. C. K. *Phys. Rev. E* **2004**, *69*, 011503.

(3) Sciortino, F. *Nature Mater.* **2002**, *1*, 145–146.

(4) Laurati, M.; Petekidis, G.; Koumakis, N.; Cardinaux, F.; Schofield, A. B.; Brader, J. M.; Fuchs, M.; Egelhaaf, S. U. *J. Chem. Phys.* **2009**, *130*, 13497.

(5) Shah, S. A.; Chen, Y.-L.; Ramakrishnan, S.; Schweizer, K. S.; Zukoski, C. F. *J. Phys.: Condens. Matter* **2003**, *15*, 4751.

(6) Shah, S. A.; Chen, Y. L.; Schweizer, K. S.; Zukoski, C. F. *J. Chem . Phys.* **2003**, *118*, 3350.

(7) Stiakakis, E.; Vlassopoulos, D.; Likos, C. N.; Roovers, J.; Meier, G. *Phys. Rev. Lett.* **2002**, *89*, 208302.

(8) Eckert, T.; Bartsch, E. *J. Phys.: Condens. Matter* **2004**, *16*, S4937–S4950.

(9) Cloitre, M.; Borrega, R.; Leibler, L. *Phys. Rev. Lett.* **2000**, *85*, 4819.

(10) Cloitre, M. Chapter titled "Yielding, Flow, and Slip in Microgel Suspensions: From Microstructure to Macroscopic Rheology". In *Microgel Suspensions: Synthesis, Properties and Applications*; Fernandez, A., Mattsson, J., Wyss, H. M., Weitz, D. A., Eds.; Wiley & Sons: New York, 2011.

(11) Vlassopoulos, D.; Fytas, G. *Adv. Polym. Sci.* **2010**, *236*, 1–54.

(12) Likos, C. N. *Phys. Rev. Lett.* **1998**, *80*, 4450.

(13) Stiakakis, E.; Vlassopoulos, D.; Roovers, J. *Langmuir* **2003**, *19*, 6645.

(14) Wilk, A.; Huissmann, S.; Stiakakis, E.; Kohlbrecher, J.; Vlassopoulos, D.; Likos, C. N.; Meier, G.; Dhont, J. K. G.; Petekidis, G.; Vavrin, R. *Eur. Phys. J. E* **2010**, *032*, 127–134.

(15) Stiakakis, E.; Petekidis, G.; Vlassopoulos, D.; Likos, C. N.; Iatrou, H.; Hadjichristidis, N.; Roovers, J. *Eur. Phys. Lett.* **2005**, *72*, 664.

(16) Kumar, S. K.; Krishnamoorti, R. *Ann. Rev. Chem. Biomol. Eng.* **2010**, *1*, 3758.

(17) Krishnamoorti, R.; Vaia, R. A. *J. Polym. Sci., Polym. Phys.* **2007**, *45*, 3252.

(18) Xu, L.; Nakajima, H.; Manias, E.; Krishnamoorti, R. *Macromolecules* **2009**, *42*, 3795.

(19) Roovers, J.; Zhouj, L.-L.; Toporowski, P. M.; van der Zwan, M.; Iatrou, H.; Hadjichristidis, N. *Macromolecules* **1993**, *26*, 4324.

(20) Gauthier, M.; Munam, A. *Macromolecules* **2010**, *43*, 3672.

(21) Roovers, J. *Polym. J.* **1986**, *18*, 153.

(22) Helgeson, E. M.; Wagner, N. J.; Vlassopoulos, D. *J. Rheol.* **2007**, *51* (2), 297–316.

(23) Erwin, B. M.; Cloitre, M.; Gauthier, M.; Vlassopoulos, D. *Soft Matter* **2010**, *6*, 2825–2833.

(24) Rogers, S.; Erwin, B. M.; Vlassopoulos, D.; Cloitre, M. *J. Rheol.* **2011**, *55*, 435.

(25) Mason, T. G.; Weitz, D. A. *Phys. Rev. Lett.* **1995**, *75*, 2770.

(26) de Gennes, P. G. *Scaling Concept in Polymer Physics*; Cornell University Press: Ithaca, NY, 1979.

(27) Gohr, K.; Schärtl, W.; Willner, L.; Pyckhout-Hintzen, W. *Macromolecules* **2002**, *35*, 9110.

(28) Berney, C. V.; Cheng, P.-L.; Cohen, R. E. *Macromolecules* **1988**, *21*, 2235.

(29) Shull, K. R. *Macromolecules* **1996**, *29*, 2659.

(30) Lindenblatt, G.; Schärtl, W.; Pakula, T.; Schmidt, M. *Macromolecules* **2001**, *34*, 1730.

(31) Likos, C. N. *Phys. Rep.* **2001**, *348*, 267–439.

(32) Flory, P. J. *J. Chem. Phys.* **1949**, *17*, 303.

(33) Flory, P. J. *Principles of Polymer Chemistry*; Cornell University Press: Ithaca, NY, 1953.
(34) Doi, M.; Edwards, S. F. *The Theory of Polymer Dynamics*; Oxford University Press: Oxford, 1986.
(35) Camargo, M.; Likos, C. N. *Phys. Rev. Lett.* **2010**, *104*, 178301.
(36) Ohta, T.; Oono, Y. *Phys. Lett. A* **1982**, *89*, 460.
(37) Likos, C. N.; Lowen, H.; Poppe, A.; Willner, L.; Roovers, J.; Cubitt, B.; Richter, D. *Phys. Rev. E* **1998**, *58*, 6299.
(38) Li, X.; Ma, X.; Huang, L.; Liang, H. *Polymer* **2005**, *45*, 6507.
(39) Li, Y.; Mattice, W. L. *Macromolecules* **1992**, *25*, 4942–4947.
(40) Miyazaki, K.; Wyss, H. M.; Weitz, D. A.; Reichman, D. R. *Eur. Phys. Lett.* **2006**, *75* (6), 915–921.
(41) Brader, J. M.; Siebenbürger, M.; Ballauff, M.; Reinheimer, K.; Wilhelm, M.; Frey, S. J.; Weysser, F.; Fuchs, M. *Phys Rev. E* **2010**, *82*, 061401.
(42) Tirtaatmadja, V.; Tam, K. C.; Jenkins, R. D. *Macromolecules* **1997**, *30*, 3271.
(43) Erwin, B. M.; Cloitre, M.; Vlassopoulos, D.; Cloitre, M. *J. Rheol.* **2010**, *54*, 915.
(44) Rogers, S. A.; Callaghan, P. T.; Petekidis, G.; Vlassopoulos, D. *J. Rheol.* **2010**, *54*, 133.
(45) Altmann, N.; Cooper-White, J. J.; Dunstan, D. E.; Stokes, J. R. *J. Non-Newtonian Fluid Mech.* **2004**, *124*, 129.
(46) Mason, T. G.; Bibette, J.; Weitz, D. A. *Phys. Rev. Lett.* **1995**, *75*, 2051.
(47) Wyss, H. M.; Miyazaki, K.; Mattson, J.; Zhibing, H.; Reichman, D. R.; Weitz, D. A. *Phys. Rev. Lett.* **2007**, *98*, 238303.
(48) Sollich, P. *Phys. Rev. E* **1998**, *58*, 738.
(49) Camargo, M.; Likos, C. N. *J. Chem. Phys.* **2009**, *130*, 204904.
(50) Pusey, P. N.; Pirie, A. D.; Poon, W. C. K. *Physica A* **1993**, *201*, 322–331.
(51) de Hoog, E. H. A.; Kegel, W. K.; van Blaaderen, A.; Lekkerkerker, H. N. W. *Phys. Rev. E* **2001**, *64*, 021407.
(52) Buzzaccaro, S.; Rusconi, R.; Piazza, R. *Phys. Rev. Lett.* **2007**, *99*, 098301.
(53) Lu, P. J.; Zaccarelli, E.; Ciulla, F.; Schofield, A. B.; Sciortino, F.; Weitz, D. A. *Nature* **2008**, *453*, 499–503.